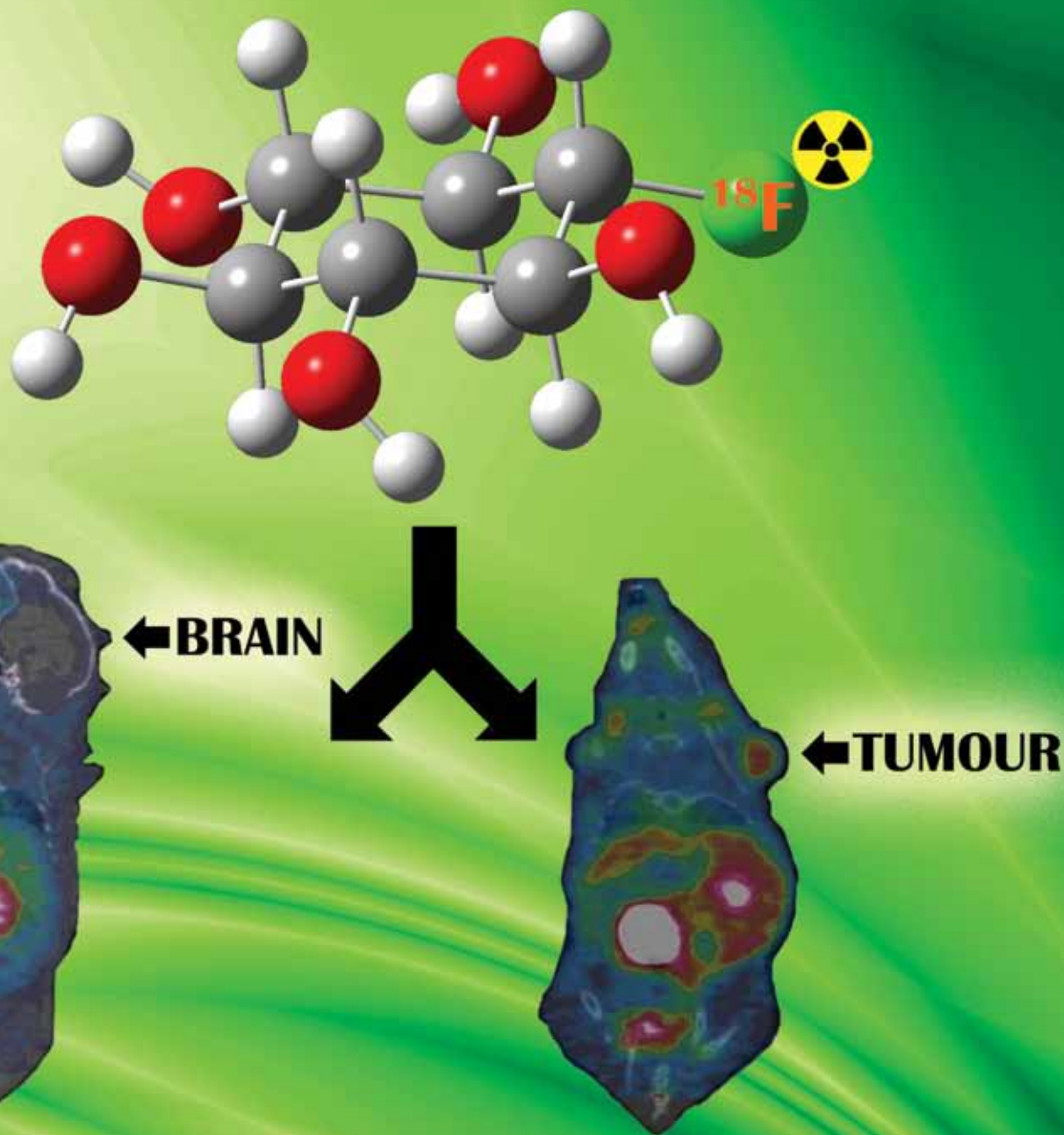


ChemComm

Chemical Communications

www.rsc.org/chemcomm

Number 37 | 7 October 2009 | Pages 5465–5644



ISSN 1359-7345

COMMUNICATION

Neil Vasdev *et al.*
Synthesis and preliminary biological evaluations of [^{18}F]-1-deoxy-1-fluoro-scyllo-inositol

FEATURE ARTICLE

Min Shi *et al.*
Recent extensions of the Morita-Baylis-Hillman reaction

RSC Publishing

Synthesis and preliminary biological evaluations of [¹⁸F]-1-deoxy-1-fluoro-*scyllo*-inositol†

Neil Vasdev,^{*ab} Jason Chio,^c Erik M. van Oosten,^{ac} Mark Nitz,^c JoAnne McLaurin,^d Douglass C. Vines,^{ef} Sylvain Houle,^{ab} Raymond M. Reilly^g and Alan A. Wilson^{ab}

Received (in College Park, MD, USA) 6th July 2009, Accepted 22nd July 2009

First published as an Advance Article on the web 11th August 2009

DOI: 10.1039/b913317h

A novel PET radiotracer, [¹⁸F]-1-deoxy-1-fluoro-*scyllo*-inositol, was synthesized via a one-pot reaction in 16 ± 3% uncorrected radiochemical yield within 80 minutes; although this compound revealed low brain penetration it shows promise in rodent tumour models for breast cancer imaging.

scyllo-Inositol (Fig. 1a) is a naturally occurring stereoisomer of inositol. Recent advances in our laboratories have revealed that *scyllo*-inositol interacts with Aβ₁₋₄₂ peptides,¹⁻³ considered to be a neurotoxic component of senile plaques deposited in patients suffering from Alzheimer's disease (AD). This compound is emerging as a promising therapeutic for AD and is presently in phase II of clinical trials. *scyllo*-Inositol may also be a new marker for breast cancer, as it has been detected in human breast tumour extracts.⁴ Given the high socioeconomic burden of AD and breast cancer there is a critical need for new methods to enable early diagnosis, to monitor disease progression and to evaluate drug therapies for these illnesses.

Extensive efforts are underway to develop radiopharmaceuticals for medical imaging with positron emission tomography (PET)⁵⁻⁷ for both AD^{8,9} and breast cancer,¹⁰ however, the existing radiopharmaceuticals for these targets require significant improvements to be reliable for early and accurate detection. *scyllo*-Inositol derivatives would represent a new class of PET radiopharmaceuticals for these illnesses.

Despite the extensive efforts, there are still no ideal PET radiopharmaceuticals for imaging AD labelled with the desirable isotope fluorine-18 (¹⁸F; *t*_{1/2} = 109.7 min, β⁺ 97%). A fluorinated analog, 1-deoxy-1-fluoro-*scyllo*-inositol

(4; Fig. 1b), was shown by our group to be effective at blocking Aβ₁₋₄₂ aggregation *in vitro*.¹¹ The objectives of the present work were to radiolabel 4 with ¹⁸F and evaluate this new PET radiopharmaceutical for potential use in imaging the central nervous system and human breast cancer xenografts in rodents.

Transformation of *scyllo*-inositol to the [¹⁸F]-labelled derivative, [¹⁸F]4, required stereoselective substitution of one hydroxyl group for a fluorine atom. A one-pot, three-step reaction was developed to prepare [¹⁸F]4 (Scheme 1), using the multi-functionalized precursor, 1,6:3,4-bis-[*O*-(2,3-dimethoxybutane-2,3-diyl)]-2-*O*-trifluoromethanesulfonyl-5-*O*-benzoyl-*myo*-inositol¹¹ (1). Compound 1 was reacted with azeotropically dried potassium cryptand fluoride ([K₂₂₂][¹⁸F]). Conversion to [¹⁸F]2 yielded a high specific activity product (10.7 Ci mmol⁻¹). Fluorine-18 labelled 2 was reacted with 40% trifluoroacetic acid (TFA) in acetonitrile to hydrolyze the diacetals to produce [¹⁸F]3. The reaction mixture was evaporated to dryness with nitrogen gas, followed by addition of 2N sodium hydroxide to hydrolyze the benzoyl group. Each step in this reaction sequence was carried out at 90 °C for 15 min and monitored by radio-HPLC and radio-TLC. Solid-phase purification and formulation of [¹⁸F]4 was achieved by passing the crude mixture through anion exchange, C-18, and alumina cartridges, connected in series, and filtering the solution into a sterile dose vial containing sodium bicarbonate and concentrated saline. The radiosynthesis of [¹⁸F]4 was accomplished in 80 min, with an uncorrected radiochemical yield of 16 ± 3% (*n* = 6) and >98% radiochemical purity at the end of synthesis (Fig. 2). It is noteworthy that our group and others have recently published proceedings describing the synthesis of [¹⁸F]4.¹²⁻¹⁴ Our procedure gave the highest radiochemical yield of [¹⁸F]4, and is attributed to the stability of the precursor, 1. The measured log*D* of [¹⁸F]4 was -2.8 ± 0.3, as determined using an established procedure.¹⁵

The non-radioactive intermediates were prepared as analytical standards using literature procedures.¹¹ Although 3 was not previously isolated, it was readily synthesized by hydrolysis of the diacetals on 2-*O*-benzoyl-1,6:3,4-bis-[*O*-(2,3-dimethoxybutane-2,3-diyl)]-5-fluoro-*scyllo*-inositol (2)¹¹ with 95% TFA. Further characterization of [¹⁸F]4 was achieved

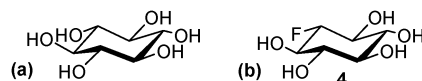


Fig. 1 Chemical structures of (a) *scyllo*-inositol and (b) 1-deoxy-1-fluoro-*scyllo*-inositol (4).

^a PET Centre, Centre for Addiction and Mental Health, 250 College St., Toronto, ON, Canada M5T 1R8.

E-mail: neil.vasdev@camhpet.ca; Fax: +1-416-979-4656; Tel: +1-416-535-8501 ext. 4680

^b Department of Psychiatry, University of Toronto, Toronto, ON, Canada M5T 1R8

^c Department of Chemistry, University of Toronto, Toronto, ON, Canada M5S 1A1

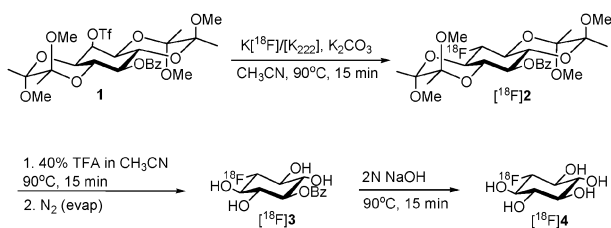
^d Centre for Research in Neurodegenerative Diseases, University of Toronto, Toronto, ON, Canada M5S 3H2

^e STTARR Innovation Centre, Radiation Medicine Program., Princess Margaret Hospital, Toronto, ON, Canada M5G 1L7

^f Department of Radiation Oncology, University of Toronto, Toronto, ON, Canada M5S 3E2

^g Leslie Dan Faculty of Pharmacy, University of Toronto, Toronto, ON, Canada M5S 3M2

† Electronic supplementary information (ESI) available: Experimental details for synthesis and characterization of 3, ¹⁹F NMR spectrum of 4, radiosynthesis and characterization of [¹⁸F]4, and biological studies. See DOI: 10.1039/b913317h



Scheme 1 Synthesis of $[^{18}\text{F}]\mathbf{4}$.

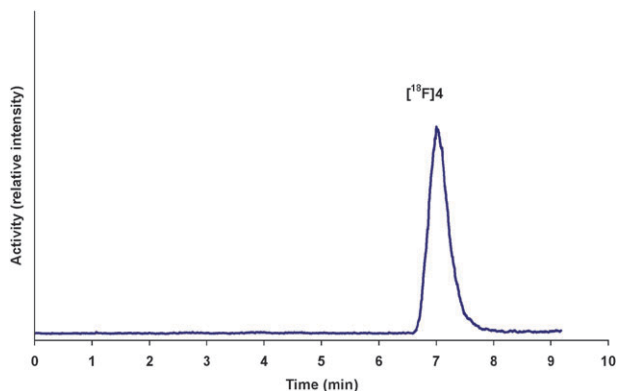


Fig. 2 Radio-HPLC chromatogram of $[^{18}\text{F}]\mathbf{4}$ after purification. Radio-HPLC conditions: mobile phase = 80 : 20 CH_3CN to H_2O ; flow rate = 2.0 mL min^{-1} ; column = Phenomenex Analytical Luna NH_2 250 \times 4.6 mm (5 μm), $\lambda = 254 \text{ nm}$.

by a “carrier-added” reaction. The radiosynthesis was repeated as above with the addition of 100 μg KF (5 : 1 mole equivalent of $\mathbf{1}$: KF) prior to the azeotropic drying step. This reaction produced $[^{18}\text{F}]\mathbf{4}$ in 11% radiochemical yield (uncorrected). The final product was co-spotted with authentic $\mathbf{4}$ and analyzed by radio-TLC in conjunction with a phosphomolybdic acid stain (R_f 0.6). The process was repeated with KF as the only source of fluorine and the ^{19}F NMR spectrum of the combined purified product conformed to that of authentic $\mathbf{4}$.

Small animal imaging studies were conducted continuously over 2 hours (dynamic scans) in female CD1 nude mice following tail vein injection of $[^{18}\text{F}]\mathbf{4}$. Mice were fasted for 12 h prior to imaging under isoflurane anaesthesia. Dynamic imaging revealed that $[^{18}\text{F}]\mathbf{4}$ had very low brain penetration and accumulated primarily in the kidneys (representative image shown in Fig. 3a). In order to confirm this finding, we carried out a preliminary cerebral *ex vivo* biodistribution study in conjunction with an *in vivo* SIC (Sonde IntraCérébrale; a β -sensitive intracerebral probe) study following tail vein injection of $[^{18}\text{F}]\mathbf{4}$ in rats.¹⁶

Ex vivo biodistribution studies in conscious male Sprague-Dawley rats further confirmed that $[^{18}\text{F}]\mathbf{4}$ has negligible brain penetration ($<0.1\%$ injected dose per gram of wet tissue (% i.d. g^{-1})) in cortex, cerebellum and rest of brain at 3 and 30 min post-injection of the radiotracer, without correction for the vascular compartment. Whole blood levels were 0.8% and 0.5% i.d. g^{-1} at the same time points, respectively. The SIC probe study was conducted from 0 to 40 min to measure radioactivity in two localized areas of the rat brain (cerebellum and frontal cortex) and showed similar results ($<0.2\%$ i.d. g^{-1}

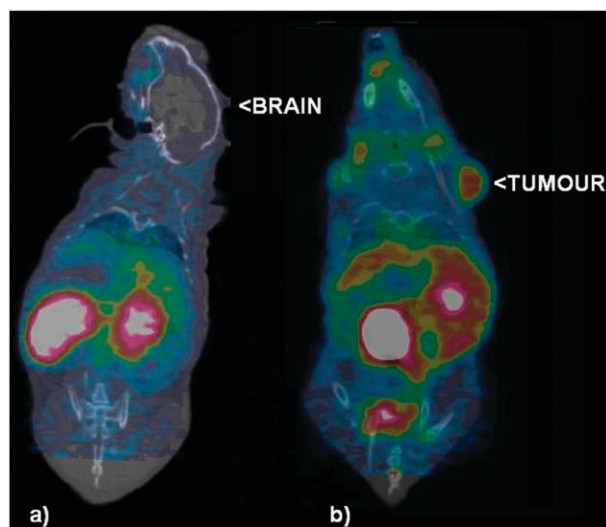


Fig. 3 Coronal PET-CT fused images of representative athymic mice implanted subcutaneously in the right shoulder with MDA-MB-231 human breast cancer xenografts 14 days post-inoculation and following tail vein injection of $[^{18}\text{F}]\mathbf{4}$. (a) Image through the plane of the brain at 3 min reveals no brain penetration and only high uptake in the kidneys; (b) image through the plane of tumour at 45 min (peak) reveals 4.5% i.d. g^{-1} in the tumour. Image intensities were adjusted for optimal delineation of volumes-of-interest and not for equivalent visualization.

at all time points). Successful radiotracers for imaging the central nervous system typically express $\geq 0.5\%$ i.d. g^{-1} of tissue in rodent brain.¹⁷ The data confirmed that $[^{18}\text{F}]\mathbf{4}$ does not readily pass the blood brain barrier and is unlikely to be useful for imaging the central nervous system.

A preliminary small animal imaging study was carried out to investigate the potential use of $[^{18}\text{F}]\mathbf{4}$ for detection of human breast cancer xenografts (MDA-MB-231 cell line) in athymic mice (Fig. 3b). Dynamic scans revealed that tumour uptake peaked at 45 min post tail vein injection of $[^{18}\text{F}]\mathbf{4}$, with 4.5% i.d. g^{-1} . The uptake of $[^{18}\text{F}]\mathbf{4}$ is similar to that of $[^{18}\text{F}]\mathbf{2}$ -fluoro-2-deoxy-D-glucose (FDG), considered the “gold standard” for cancer imaging with PET, in the same xenograft tumour model ($5.5 \pm 1.7\%$ i.d. g^{-1} at 60 min post-injection) under similar experimental conditions.¹⁸ Limitations of FDG PET in the follow-up of breast cancer patients include the relatively high rate of false-positive results in patients with known or suspected malignancy, as FDG uptake in non-malignant inflammatory conditions has been observed. The rather low specificity of FDG PET may be improved by the use of $[^{18}\text{F}]\mathbf{4}$ and other inositol-based imaging agents. The development of several new $[^{18}\text{F}]\mathbf{4}$ -labelled inositol derivatives, optimization and automation of the radiochemistry, and continued oncology imaging studies are currently under way in our laboratories.

This study was conducted with the support of the Natural Sciences and Engineering Research Council and Canadian Institutes for Health Research (CHRPJ 365537-2009), a Young Investigators Grant from the Alzheimer’s Society of Canada (M.N.) as well as the Ontario Institute for Cancer Research through funding provided by the Government of Ontario. All animal experiments were carried out under

humane conditions, with approval from the Animal Care Committee at the Centre for Addiction and Mental Health or the University Health Network and in accordance with the guidelines set forth by the Canadian Council on Animal Care. The authors thank Armando Garcia and Winston Stableford for fluorine-18 production as well as Dr David Green, Dr Jun Parkes, Patrick McCormick, and Kristin McLarty for helpful discussions and their expertise with the biological studies.

Notes and references

- 1 D. Fenili, M. Brown, R. Rappaport and J. McLaurin, *J. Mol. Med.*, 2007, **85**, 603–611.
- 2 J. McLaurin, M. E. Kierstead, M. E. Brown, C. A. Hawkes, M. H. Lambermon, A. L. Phinney, A. A. Darabie, J. E. Cousins, J. E. French, M. F. Lan, F. Chen, S. S. Wong, H. T. Mount, P. E. Fraser, D. Westaway and P. St George-Hyslop, *Nat. Med. (N. Y.)*, 2006, **12**, 801–808.
- 3 M. Nitz, D. Fenili, A. A. Darabie, L. Wu, J. E. Cousins and J. McLaurin, *FEBS J.*, 2008, **275**, 1663–1674.
- 4 I. S. Gribbestad, S. B. Petersen, H. E. Fjosne, S. Kvinnsland and J. Krane, *NMR Biomed.*, 1994, **7**, 181–194.
- 5 S. M. Ametamey, M. Honer and P. A. Schubiger, *Chem. Rev.*, 2008, **108**, 1501–1516.
- 6 L. S. Cai, S. Y. Lu and V. W. Pike, *Eur. J. Org. Chem.*, 2008, 2853–2873.
- 7 P. W. Miller, N. J. Long, R. Vilar and A. D. Gee, *Angew. Chem., Int. Ed.*, 2008, **47**, 8998–9033.
- 8 J. R. Barrio, N. Satyamurthy, S. C. Huang, A. Petric, G. W. Small and V. Kepe, *Acc. Chem. Res.*, 2009, **42**, 842–850.
- 9 W. E. Klunk and C. A. Mathis, *Curr. Opin. Neurol.*, 2008, **21**, 683–687.
- 10 K. McLarty and R. M. Reilly, *Clin. Pharmacol. Ther.*, 2007, **81**, 420–424.
- 11 Y. Sun, G. Zhang, C. A. Hawkes, J. E. Shaw, J. McLaurin and M. Nitz, *Bioorg. Med. Chem.*, 2008, **16**, 7177–7184.
- 12 K. Pal, U. Mukhopadhyay, A. Volgin, A. Sharvin, W. P. Tong, J. G. Gelovani and M. M. Alauddin, Proceedings of the 56th Annual Meeting of the Society of Nuclear Medicine, Toronto, 2009, *J. Nucl. Med.*, 2009, **50**, 68P.
- 13 T. M. Shoup, D. R. Elmaleh, E. A. Carter, D. A. Winter, C. R. Tolman and A. J. Fischman, Proceedings of the 56th Annual Meeting of the Society of Nuclear Medicine, Toronto, 2009, *J. Nucl. Med.*, 2009, **50**, 410P.
- 14 N. Vasdev, P. V. Kulkarni, E. M. van Oosten, P. Cao, J. Chio, M. Nitz, J. McLaurin, S. Houle and A. A. Wilson, Proceedings of the 56th Annual Meeting of the Society of Nuclear Medicine, Toronto, 2009, *J. Nucl. Med.*, 2009, **50**, 68P.
- 15 A. A. Wilson, L. Jin, A. Garcia, J. N. DaSilva and S. Houle, *Appl. Radiat. Isot.*, 2001, **54**, 203–208.
- 16 N. Vasdev, S. Natesan, L. Galineau, A. Garcia, W. T. Stableford, P. McCormick, P. Seeman, S. Houle and A. A. Wilson, *Synapse (N. Y.)*, 2006, **60**, 314–318.
- 17 D. F. Wong and M. G. Pomper, *Mol. Imaging Biol.*, 2003, **5**, 350–362.
- 18 K. McLarty, A. Fasih, D. A. Scollard, S. J. Done, D. C. Vines, D. E. Green, D. L. Contantini and R. M. Reilly, *J. Nucl. Med.*, submitted.